Hydrology Research

British Hydrological Society

IWA PUBLISHING

Hydrology Research Vol 54 No 3, 382 doi: 10.2166/nh.2023.130

Spatio-temporal characteristics and driving factors of the meteorological drought across China based on CMIP6

Mengru Zhang [a,b], Xiaoli Yang[a,b,*], Ming Pan[c], Linyan Zhang[a,b], Xiuqin Fang[a,b] and Justin Sheffield[d]

[a] State Key Laboratory of Hydrology-Water Resources and Hydraulic Engineering, Hohai University, Nanjing, China
[b] College of Hydrology and Water Resources, Hohai University, Nanjing, China
[c] Center for Western Weather and Water Extremes, Scripps Institution of Oceanography, University of California San Diego, La Jolla, CA, USA
[d] Geography and Environment, University of Southampton, Southampton, UK
*Corresponding author. E-mail: yangxl@hhu.edu.cn

MZ, 0000-0001-7689-0917

ABSTRACT

The characteristics of meteorological drought in different river basins in China have clear spatio-temporal differences and the difference between watersheds is also reflected in the influence mechanism of meteorological drought. This study investigated the meteorological drought risk under different future emission scenarios, based on the Coupled Model Intercomparison Project 6 (CMIP6). Furthermore, we explored the influence of precipitation and temperature on meteorological drought in different basins of China in the future. Meanwhile, the uncertainty associated with CMIP6 in different watersheds is also considered. In the future, the frequency of meteorological drought events mainly shows a decreasing trend, but the drought intensity and duration increase. In China, the rate of probability change in drought's intensity was greater than drought duration and the probability distribution of drought characteristics is significantly different between the historical and the future periods. Under the low and medium emission scenarios (SSP126 and SSP245), the Joint Recurrence Period of future drought intensity and duration increases and the Recurrence Period decreases in the western and north-eastern basins. Precipitation plays a major role in the meteorological drought, especially in the northeast and southeast basins of China.

Key words: CMIP6, copula, meteorological drought, return period, SC-PDSI, uncertainty

HIGHLIGHTS

- The meteorological drought intensity and duration will increase in the western basin.
- The probability of drought intensity increases faster than the duration of drought.
- The JRP of bivariate drought will be a mainly increasing trend in the future.
- The driving factor of a meteorological drought is different in China and precipitation is more prominent than temperature.

GRAPHICAL ABSTRACT

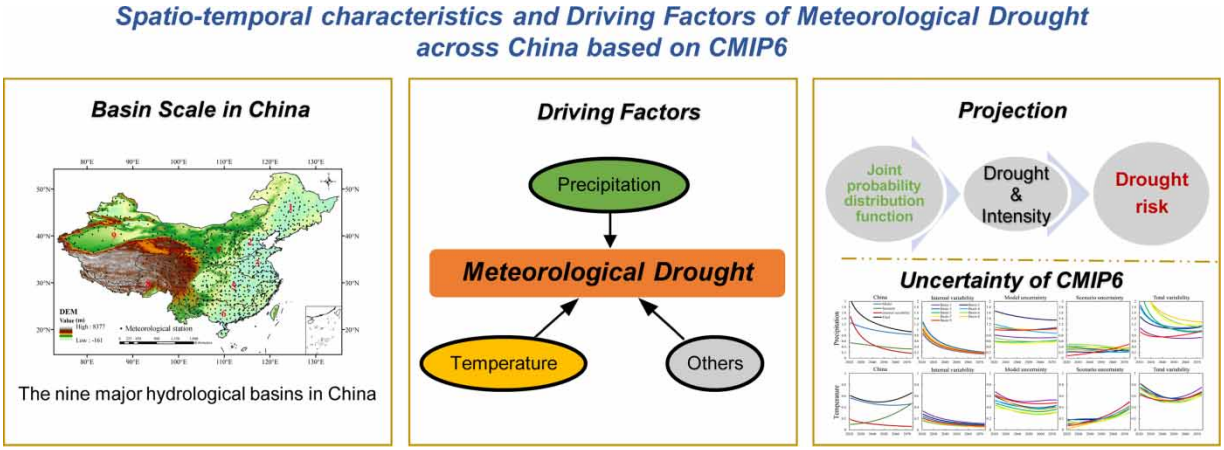

1. INTRODUCTION

Drought is a kind of natural disaster, usually having a substantial impact on the national economy, society and ecological environment. Therefore, people attach great importance to drought research. In the context of global warming, droughts have been exacerbated by climate change so far and have led to significant changes in the areas impacted by droughts worldwide (Samaniego *et al.* 2018). Usually, drought arises from a severe precipitation deficiency and is described in terms of changes in major meteorological factors (such as precipitation and temperature) and anomalies compared to long-term averages (Yang *et al.* 2020). The Intergovernmental Panel on Climate Change (IPCC) Fifth and Sixth Assessment Reports concluded that the climate system is getting warmer on the global scale (IPCC 2021). Under the effects of climate warming, the evolution and mechanism of drought have become an increasingly important research topic. Therefore, exploring predicted changes in drought characteristics under different emission scenarios will help formulate disaster prevention and mitigation policies.

Usually, there are four major types of droughts: agricultural drought (Heim 2002), socioeconomic drought (Shukla & Wood 2008), hydrological drought (Mishra & Singh 2011) and meteorological droughts (Hayes *et al.* 2011). Due to the availability of relatively long historical data for observations of meteorological variables, meteorological drought is one of the most extensively studied droughts (Harris *et al.* 2014). A lot of studies on meteorological drought indicators have been carried out. The most commonly used methods are the Standardized Precipitation Index (SPI) (Mckee *et al.* 1993), the Standardized Precipitation Evapotranspiration Index (SPEI) (Vicente-Serrano *et al.* 2010) and the Palmer Drought Severity Index (PDSI) (Palmer 1965). The SPI only considers precipitation and ignores the influence of temperature on meteorological drought. The SPEI responds very differently to precipitation and temperature of different climates and locations and it relies highly on temperature. The PDSI is the index that is most widely applied to meteorological drought and is most suitable to assess the impact of global warming on drought, which incorporates precipitation and temperature. The PDSI can adjust and balance the contributions of precipitation and temperature to local water anomalies for different climate conditions, implying better spatio-temporal consistency and comparability. Meanwhile, Wells *et al.* (2004) found a new algorithm for calculating PDSI, named the Self-Calibrating PDSI (SC-PDSI). Based on the historical meteorological observation data of a single station, the SC-PDSI can determine the climate parameters applicable to the local area. The SC-PDSI has better spatial and temporal stability and comparability than the earlier PDSI. Therefore, we chose the SC-PDSI to investigate the spatio-temporal characteristics of meteorological drought.

The General Circulation Models (GCMs) are generally used for meteorological drought projection, which is published by the Coupled Model Intercomparison Project (CMIP). CMIP6 is considered advantageous over CMIP3 and CMIP5 in reproducing temperature and precipitation patterns (Bock *et al.* 2020). In particular, CMIP6 is advantageous in capturing precipitation features (Na *et al.* 2020). Therefore, we used the precipitation and temperature data in the latest CMIP6 for predicting meteorological drought. Precipitation and temperature, as the data of the SC-PDSI calculation are the main influencing factors of meteorological drought. There have been many studies on the influencing factors of meteorological drought. In the midlands of the UK, researchers found that precipitation has a greater impact on meteorological drought compared to temperature (Rahmani & Fattahi 2021). However, the observed increase in precipitation in Central Europe and the Balkans is not significant; in these regions, temperature drives the increase in meteorological drought severity (Spinoni *et al.* 2015).

In China, studies on the driving factors of meteorological drought mainly focus on the El Niño Southern Oscillation (ENSO), the Pacific Decadal Oscillation (PDO), the Atlantic Oscillation (AO) and solar activity (Huang *et al.* 2016; Yue *et al.* 2022). However, there are few relevant studies on the effects of precipitation and temperature elements on the meteorological drought in China. Precipitation and temperature, as two meteorological factors, also play an important role in meteorological drought. In northeast China, Li *et al.* (2020) found that the direct effect of precipitation on meteorological drought was greater than that of other meteorological factors and the dominant driving factors were also influenced by seasons. The influence of meteorological factors on meteorological drought is very complex. Hence, considering the complex geographical environment in China, we estimate the contribution of precipitation and temperature to meteorological drought at the watershed scale and analyse the influence of the above two meteorological factors on meteorological drought in China.

In this study, we focus on the evolution and influencing mechanisms of meteorological drought at basin scales over China. The objective was to determine the trend of drought under climate change conditions using the SC-PDSI under four future scenarios (SSP126, SSP245, SSP370 and SSP585) and historical periods. We explored the leading meteorological factors of

meteorological drought and the meteorological drought risk of different river basins in China. This study is helpful for understanding and predicting drought trends in different basins around China.

2. STUDY AREA AND DATASET

2.1. Study area

This study subdivided China into nine major hydrological regions (Figure 1) due to its complex terrain and multiple climate types; these regions include the well-known Yellow River (B4) and Yangtze River Basins (B5), as well as the Songliao River (B1), Hai River (B2), Huai River (B3), Pearl River (B6), Southeast River (B7), Southwest River (B8) and Northwest River (B9) Basins. In the following sections, the nine basins above are represented by the abbreviations B1–B9.

2.2. Data

The daily precipitation and temperature observational datasets from 1961 to 2014 over China were obtained from 823 meteorological stations in the National Meteorological Information Center, the China Meteorological Administration (CMA) (http://data.cma.cn/, accessed on 20 May 2021). The meteorological station datasets cover the area ranging from 16.53°N to 53.48°N and 75.18°E to 132.96°E. The CMA has conducted quality control on the temperature data collected at all meteorological stations; the meteorological data of each meteorological station have no obvious mutations and random changes and, therefore, can represent the climate status of the research area. This study established a daily precipitation and temperature observational dataset and the spatial resolution was processed at 10 km $\times$10 km over China by the bilinear interpolation method (Gustavsson & Peetre 1977).

Based on the observed data, the performances of bias-corrected CMIP6 General Circulation Models (GCMs) for simulating a meteorological drought over China were evaluated. The models are archived at the Program on Climate Model Diagnosis and Intercomparison (PCMDI) website (https://pcmdi.llnl.gov/index.html, accessed on 10 January 2021). Limited by the daily scale CMIP6 data, 15 climate models were selected in this research (Table 1). In this research, data sets were selected as daily data. We first processed daily scale data into monthly scale data and then calculated the meteorological drought index

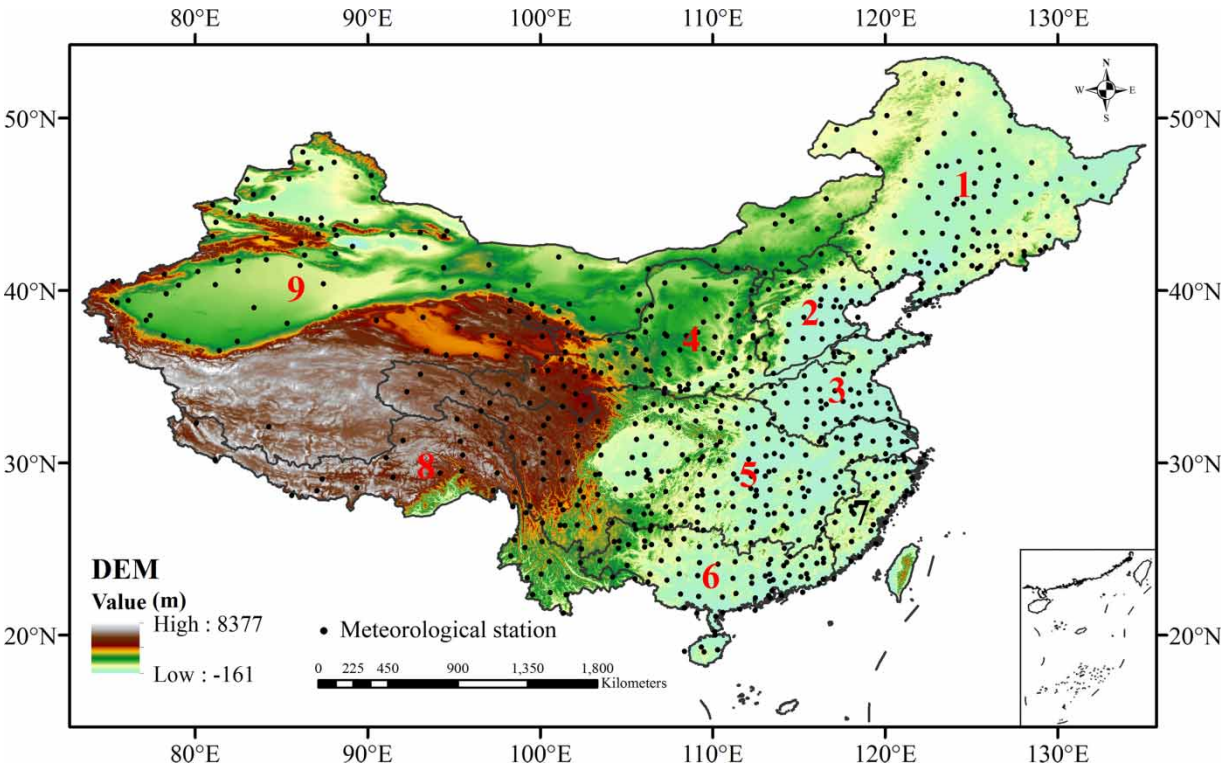

Figure 1 | Distribution of nine large river basins (B1-Songliao River, B2-Haihe River, B3-Huaihe River, B4-Yellow River, B5-Yangtze River, B6-Pearl River, B7-Southeast River, B8-Southwest River, and B9-Northwest River Basins).

Table 1 | Model names, institute and resolution information for 15 general circulation models

No.	Model name	Institute	Resolution (lon × lat)
1	ACCESS-CM2	Australia: CSIRO-ARCCSS	1.2° × 1.8°
2	ACCESS-ESM1-5	Australia: CSIRO	1.2° × 1.8°
3	BCC-CSM2-MR	China: BCC	1.12° × 1.12°
4	CanESM5	Canada: CCCma	2.8° × 2.8°
5	CESM2-WACCM	America: NCAR	0.94° × 1.25°
6	CMCC-CM2-SR5	Italy: CMCC	1.0° × 1.0°
7	FGOALS-g3	China: CAS	2.25° × 2°
8	IITM-ESM	India: CCCR-IITM	2° × 2°
9	MIROC6	Japan: MIROC	1.4° × 1.4°
10	MPI-ESM1-2-HR	Germany: MRI-M DWD DKRZ	0.9°× 0.9°
11	MPI-ESM1-2-LR	Germany: MRI-M AWI DKRZ	1.9°× 1.9°
12	MRI-ESM2-0	Japan: MRI	1.125° × 1.125°
13	NorESM2-LM	Norway: NCC	1.9° × 2.5°
14	NorESM2-MM	Norway: NCC	0.9° × 1.3°
15	TaiESM1	Taiwan in China: RCEC-AS	1.3° × 0.9°

(SC-PDSI). The reason for selecting daily scale data is to lay the foundation for further research and the CMIP6 daily dataset provides more possibilities for drought research, such as hydrological drought and its connection with meteorological drought. The historical period of CMIP6 data covers 54 years, from 1961 to 2014; therefore, the future period is selected to be from 2021 to 2074. Considering future conditions and global warming signals, four Shared Socioeconomic Pathways (SSP) scenarios (SSP126, SSP245, SSP370 and SSP585) with low, medium and high future greenhouse gas emissions were simulated and compared. All model outputs were first bilinearly-interpolated to the same 10 km × 10 km grid as the observations for the different spatial resolutions of different GCMs. In addition to precipitation and temperature data, the soil available water capacity is also required to calculate the SC-PDSI and the soil available water capacity data were obtained from the available water capacity dataset provided by Webb *et al.* (2000) in globally gridded digital format.

3. METHODOLOGIES

3.1. Bias correction

The Equidistant Cumulative Distribution Function (EDCDF) as a bias correction method (Li *et al.* 2010) was used in this research for bias correction of GCMs. It takes advantage of the difference between the cumulative distribution characteristics of climate elements simulated by GCMs and those regionally measured to correct the deviation of simulated values and effectively capture the extreme values. The EDCDF method improves the inherent errors in climate model data and the limitations of applied interpolation methods to increase the simulation accuracy of climate elements. The EDCDF has good applicability in correcting the deviation of precipitation and temperature in China (Zhang *et al.* 2021). Based on the CMA dataset, bilinear interpolation and the EDCDF method are combined to downscale and correct the precipitation and temperature of the 15 CMIP6 models (Table 1) in both historical (1961–2014) and future (2021–2074) periods.

3.2. The SC-PDSI and drought characteristics

The PDSI introduced the concept of 'Climatically Appropriate for Existing Condition' (CAFEC) precipitation (Palmer 1965), which means the minimum precipitation required to maintain normal soil moisture levels in a given area. The magnitude of CAFEC precipitation depends on local climatic conditions. The difference between actual precipitation and CAFEC precipitation can reflect the moisture departure in a given area at a given time.

A simple two-layer soil water balance model was used to calculate the actual and probable values of hydrological components, based on meteorological observed precipitation and temperature data. Meanwhile, the Possible Evapotranspiration (PET) was estimated using the Thornthwaite method based on the monthly average temperature. In addition, the PDSI was calculated by

the adaptive algorithm proposed by Wells *et al.* (2004). Table 2 shows the classification of drought according to the Palmer's recommendation.

The drought indicator S for each month is calculated as:

$$S(t, n) = \begin{cases} |\mathrm{PDSI}(t, n)| & \text{if} \quad \mathrm{PDSI}(t, n) \leq -2 \\ 0 & \text{if} \quad \mathrm{PDSI}(t, n) > -2 \end{cases} \tag{1}$$

where $S(t, n) > 0$ indicates that drought occurs at location n at time t. The duration and intensity of a drought event are calculated as:

$$Duration(n) = T_2 - T_1 \tag{2}$$

$$Intensity(n) = \frac{\left(\sum_{T_1}^{T_2} S(t, n)\right)}{Duration(n)} \tag{3}$$

where $Duration(n)$ and $Intensity(n)$ is the drought duration and intensity of drought event m at location n, T_1 and T_2 are the first and the last time steps of drought event m.

3.3. Wavelet coherence method

The wavelet coherence method (Torrence & Webster 1999) is used to analyse the driving meteorological factor of meteorological drought. The wavelet coherence method is usually referred to as the Fourier squared coherency. When comparing two variables, it is used to identify frequency bands that covary between two time series of variables. After the normalized calculation of the wavelet power spectrum, the wavelet coherence is obtained by the square of the absolute value of the wavelet coherence spectrum. This study used the wavelet coherence method to calculate the frequency band and time interval of meteorological variables.

3.4. Meteorological drought risk assessment

The return period is a method that can respond to the degree of drought risk. The application of the return period has gradually evolved from univariate to multivariate (Hao & Singh 2015). For a multivariate return period, it is usually necessary to construct joint distribution functions.

In bivariate or multivariate environments, the return period has different definitions and the Kendall distribution function or joint probability distribution function is usually used (Gräler *et al.* 2013). We used the joint probability distribution function method in this study. Two scenarios exist for such a joint return period, one in which both variables exceed the threshold and the other in which one or more variables exceed the threshold. The joint return period in the two cases can be represented by Equations (4) and (5).

$$T_{DI} = \frac{E}{P(D \geq d \text{ and } I \geq i)} = \frac{E}{1 - F_D(d) - F_I(i) + C(F_D, F_I)} \tag{4}$$

$$T'_{DI} = \frac{E}{P(D \geq d \text{ or } I \geq i)} = \frac{E}{1 - C(F_D, F_I)} \tag{5}$$

where T_{DI} and T'_{DI} represent the Joint Recurrence Period (JRP) and Recurrence Period (RP) of drought intensity and duration. The JRP represents the time interval at which the event is likely to occur when two variables are simultaneously greater than

Table 2 | Classification of drought degree for SC-PDSI

SC-PDSI value	Categories
$-2 <$ value ≤ -1	Mild dry
$-3 <$ value ≤ -2	Moderately dry
$-4 <$ value ≤ -3	Severely dry
value ≤ -4	Extremely dry

or equal to a specific threshold. When one of the variables is greater than or equal to a specific threshold, RP represents the time interval at which it is likely to occur. The D and I represent drought duration and intensity and d and i are the duration and intensity values under a given univariate return period. The P is the joint probability of two variables, the E is the expectation of drought interval and its value is the sum of the drought duration expectation and the non-drought duration expectation. The F_D and F_I are marginal distributions of drought duration and intensity. The C is the joint probability distribution of two variables.

4. RESULTS

4.1. Performance of bias correction

To evaluate the performance of the EDCDF bias-corrected method in the 15 single models and ensemble model of CMIP6, we calculated the Root Mean Square Error (RMSE) of monthly precipitation and monthly mean temperature from 1961 to 2014 (Figure 2). Figure 2 shows that the bias-corrected effect of the EDCDF method for precipitation and temperature is clear, especially for temperature. For the 15 single models and the ensemble average model, after EDCDF correction, the median

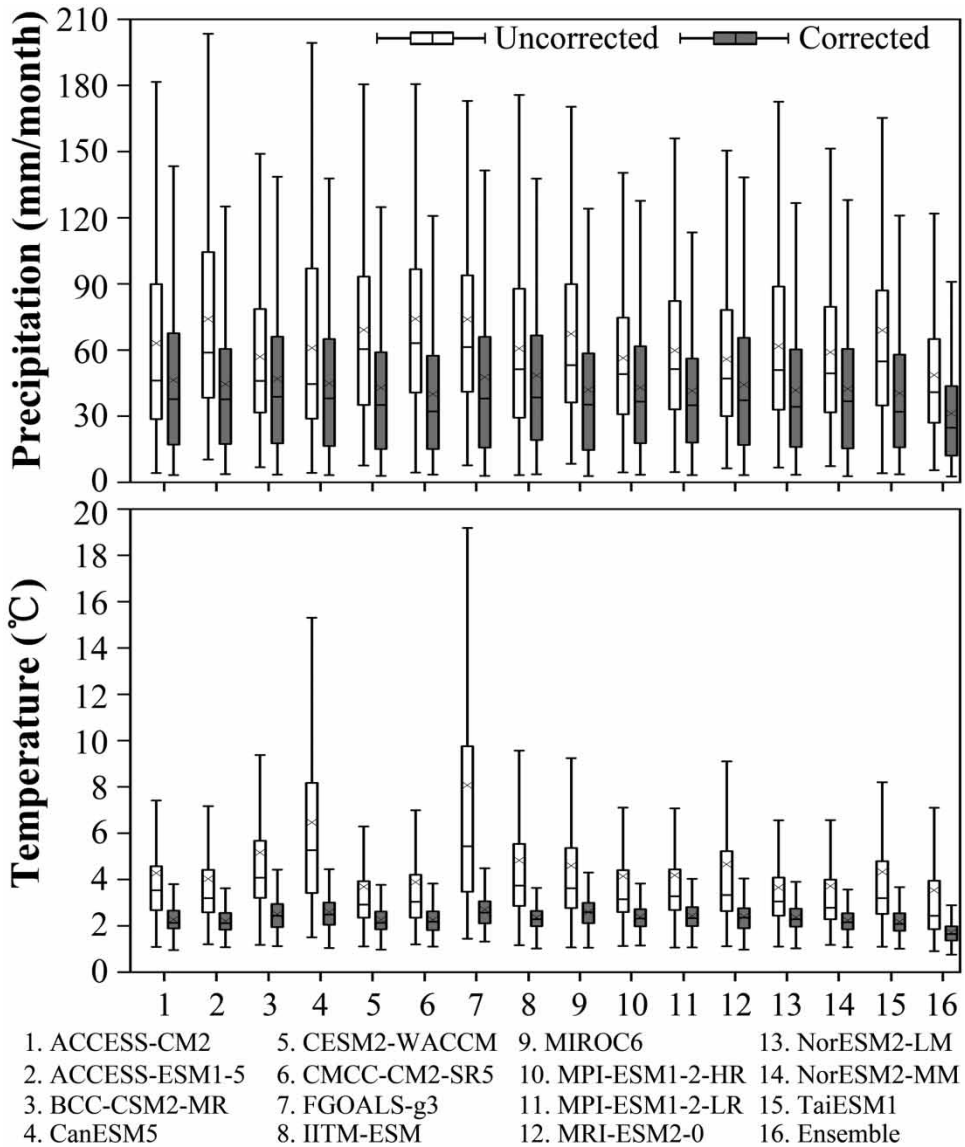

Figure 2 | RMSE of precipitation and temperature of 15 CMIP6 models and ensemble model against observations (the EDCDF bias-corrected results are represented by black box and the white represent the absence of bias correction) during 1961–2014.

RMSE of temperature and observed data decreased by approximately 1.25 °C and the median RMSE of precipitation and observation decreased by approximately 30.57 mm/month. For the ensemble model, the median RMSE of bias-corrected precipitation was 30 mm/month and the median RMSE of bias-corrected temperature was 1.65 °C. Compared to the other 15 individual models, the ensemble model had the smallest RMSE for precipitation and temperature. This shows that the multi-model ensemble can be considered as a good reference in our study for performing the bias correction of precipitation and temperature. Therefore, we chose the bias-corrected multi-model ensemble to study meteorological drought.

In order to evaluate the spatial correction effect of the ensemble model in different regions of China, the precipitation and temperature deviations from the observations were calculated (Figure 3). Figure 3 shows that the EDCDF correction method has good applicability in all basins over China. After bias correction, the precipitation deviations between the ensemble model and observations were reduced from −2 to 4% and the temperature deviation was reduced in the range of −1 to 0.1 °C. Especially in the south-eastern basins of China, the temperature and precipitation deviations from the observations decreased significantly. This indicates that the simulation accuracy of the multi-model ensemble in precipitation and temperature data is the highest in the south-eastern basins (Basins 5–7). The results may be related to the geographical location of China, which is influenced by an abundance of precipitation and small differences in temperature in the southeast, resulting in the better simulation of CMIP6-driven meteorological variables such as temperature and precipitation in this region.

4.2. Meteorological drought characteristics

To analyse meteorological drought characteristics during the historical period (from 1961 to 2014) and future period (from 2021 to 2074), the intensity and duration were selected as two drought measures. We analysed both the evolution patterns of meteorological drought characteristics in different basins in China and the risk assessment of predicted drought intensity and duration.

To analyse the trends of meteorological drought in the nine considered basins in China, Figure 4 displays the Mann-Kendall (MK) trend for drought intensity and duration in the historical and future periods. From 1961 to 2014, meteorological drought intensity and duration had a clear increasing trend. The drought intensity and duration increased significantly (95%

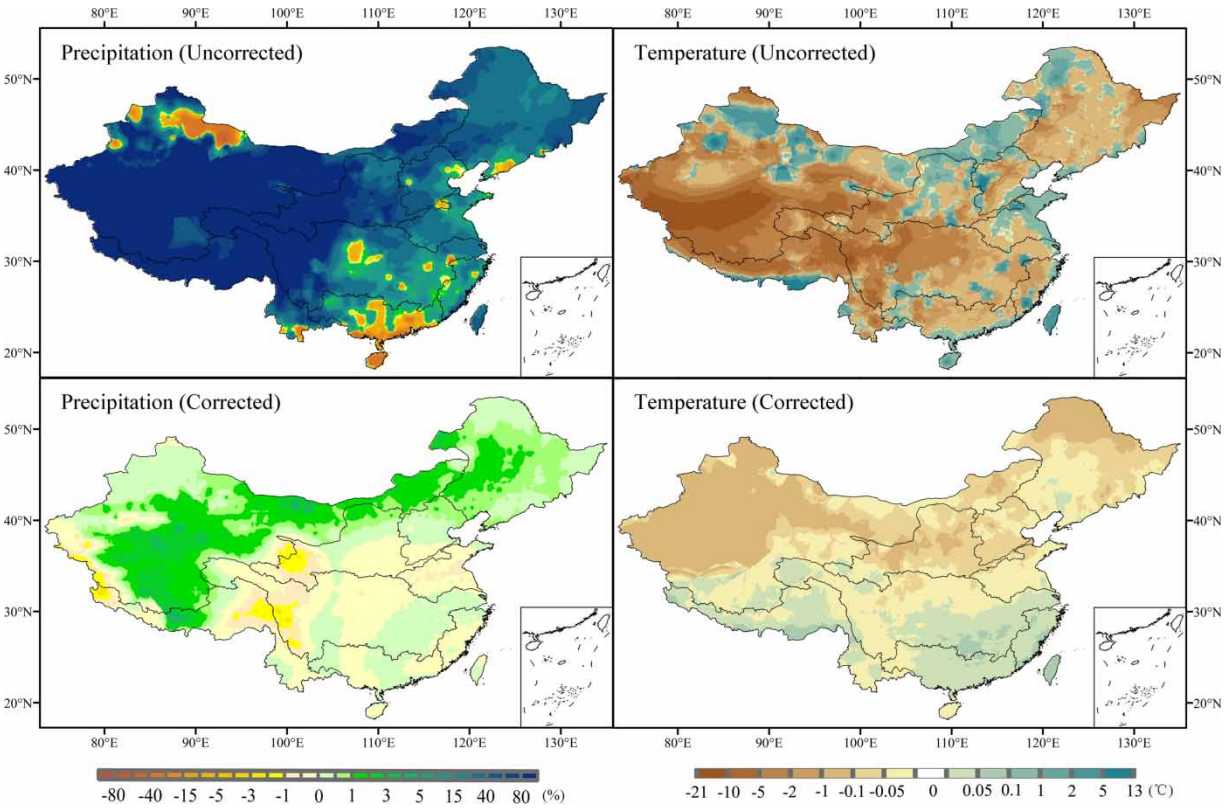

Figure 3 | Differences in precipitation and temperature of ensemble model (uncorrected and corrected results) against observations.

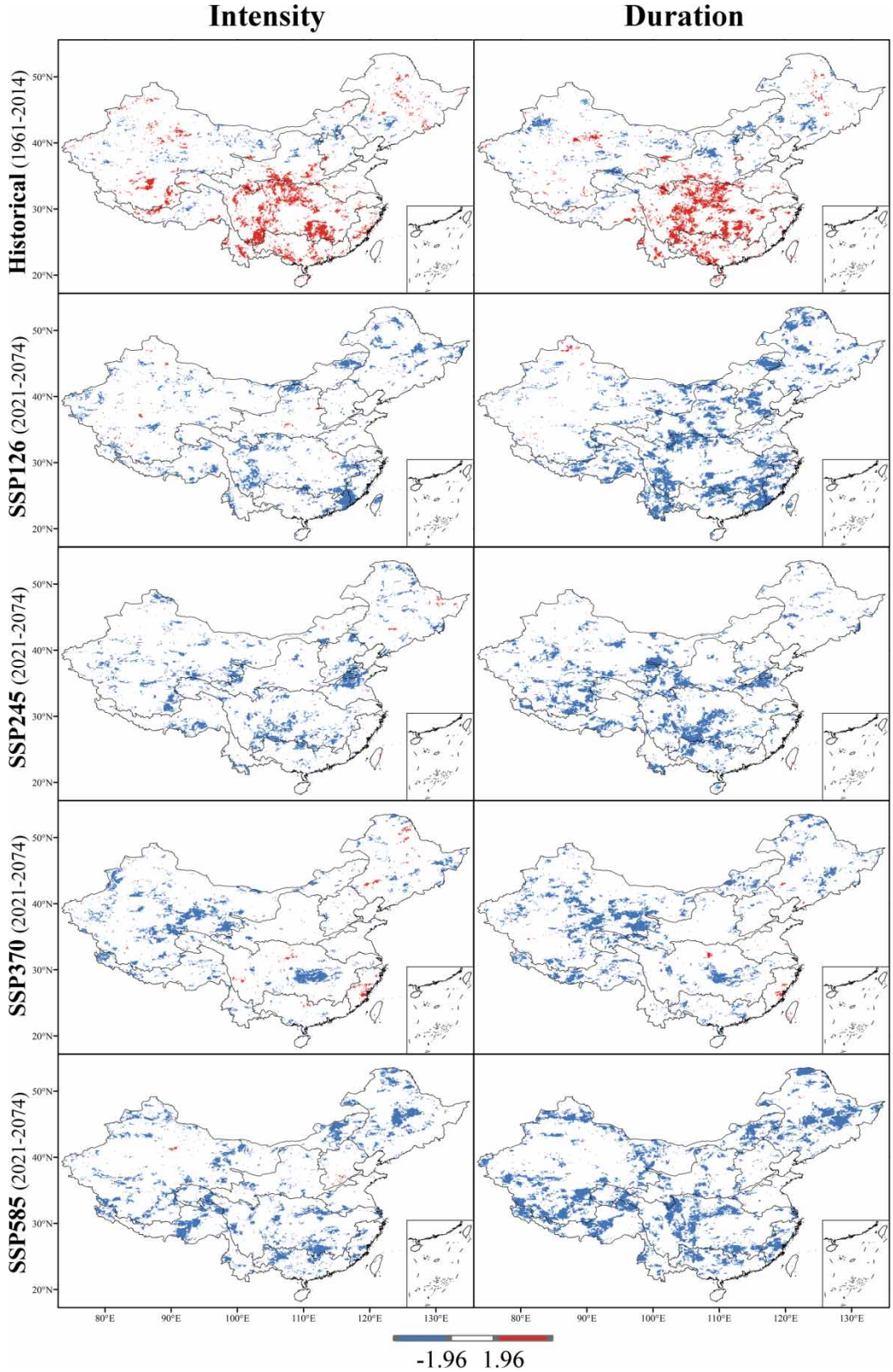

Figure 4 | MK trend of drought intensity and duration in historical (1961–2014) and future period (2021–2074) under four scenarios.

confidence level) in the southern basins (including the Yangtze River (B5), Pearl River (B6) and Southwest River (B8) basins), the northern basin (B1) and the Northwest River Basin (B9). In the future, meteorological drought intensity and duration mainly present a decreasing trend. There is a large regional meteorological drought duration with a decreasing trend, while drought intensity has a decreasing trend in a small region. For the four considered scenarios, the region with a significant decreasing trend in both drought intensity and duration was larger than that under the SSP370 scenario. Under the SSP370 scenario, the decreasing trend of both drought characteristics is expected to be mainly concentrated in the B5 and B9 basins. Under the other three scenarios, it mainly occurred in the south-eastern basins. Compared with the SSP370 scenario, most of the basins presented a clear decreasing trend under the other three future scenarios. The results show that the variation trend of meteorological drought intensity and duration is significant, mainly increasing in the historical period but decreasing significantly in the future.

To compare the regional differences in meteorological drought in historical and future periods, we calculated the percentage change in meteorological drought characteristics (intensity, duration and frequency) in future periods related to historical periods (Figure 5). The results show that: from 1961 to 2014, drought events occurred mainly in the central and northern basins, including the Yellow River (B4), Yangtze River (B5), Huaihe River (B3) and Songhua River (B1) basins. In the B1 and B5 basins, the areas with more drought events had shorter drought durations of 1–3 months and the B3 and B4 basins had drought durations of 1–6 months. Drought occurs frequently in the central region with a short drought duration and often has a low drought intensity. Except for the B4 basin, the drought intensity was relatively low in the central basins of China. Meanwhile, the northern part of the Northwest River Basin (B9) and the B1 basin had higher drought intensity and longer duration and were prone to long-duration and high-intensity drought events. For the percentage change in meteorological drought characteristics in future periods related to the historical period, in most areas, the projected change range of drought intensity is small, approximately −10 to 10%, while the absolute percentage change range of drought duration is large, more than 50%. In the future, the duration and intensity of drought events are expected to increase in some parts of the B9, Southwest River (B8) and B1 basins. However, in these regions, the frequency of drought events is expected to decrease in the future period, but the duration and intensity are expected to increase. Conversely, in some regions with an increasing number of future drought events, such as the Southeast River (B7) and B5 basins, the drought intensity and duration are expected to decrease. The spatial distribution of drought events is expected to be more concentrated with decreasing trends in the future, which include the B1, the central and western part of the B4, the western part of the B5, the central part of the B9 and the western part of the Pearl River (B6) basins. The spatial distribution of the increased intensity of future drought events is consistent with that of regions with long durations and low frequencies of drought events.

4.3. Changes in meteorological drought risk

Drought risk is also an important evaluation indicator for meteorological drought, then we analysed the return period of meteorological drought. We fit the duration and intensity distribution of each basin using five distributions, the Normal, Gamma, Weibull, Generalised Extreme Value (GEV) and Exponential (EXP) distributions. The Kolmogorov–Smirnov test (Massey 1951) is selected to test the applicability of the distribution. The results all passed the 99% confidence test. In the historical period, the optimal fitting distribution is the Weibull distribution for drought duration and intensity. In the future period, the optimal distribution of drought duration is the Weibull, Gamma and GEV distributions and the optimal distribution of intensity is the Weibull distribution. In general, the Weibull distribution is the optimal fitting distribution of the two drought characteristic variables in historical and future periods. Therefore, the Weibull distribution function was used to fit and calculate the duration and intensity of the meteorological drought in all basins.

First, in the univariate frequency analysis, we calculated the drought intensity and duration probability under two return period levels (50-year and 100-year drought levels). For the probability diagram (Figure 6), the scaling of probability values depends on the normal distribution and the probability value is the midpoint between the evaluation points of the empirical cumulative distribution function of the return period. For a given variable value x, the probability plot can represent the probability that the variable is less than x and the maximum probability is one. Figure 6 presents the probability of drought intensity and duration under the 50-year and 100-year drought levels. Under different drought return period levels (50-year and 100-year drought levels), there are differences in the univariate probability distributions. When the probability value is greater than 0.1, drought duration under 50-year drought level is 0–10 months and drought intensity is 2–3, but under the 100-year drought level, drought duration is between 0 and 20 months and drought intensity is between 2.5 and 3.8. Meanwhile, compared with historical and future periods, this is very different in the probability distribution of drought

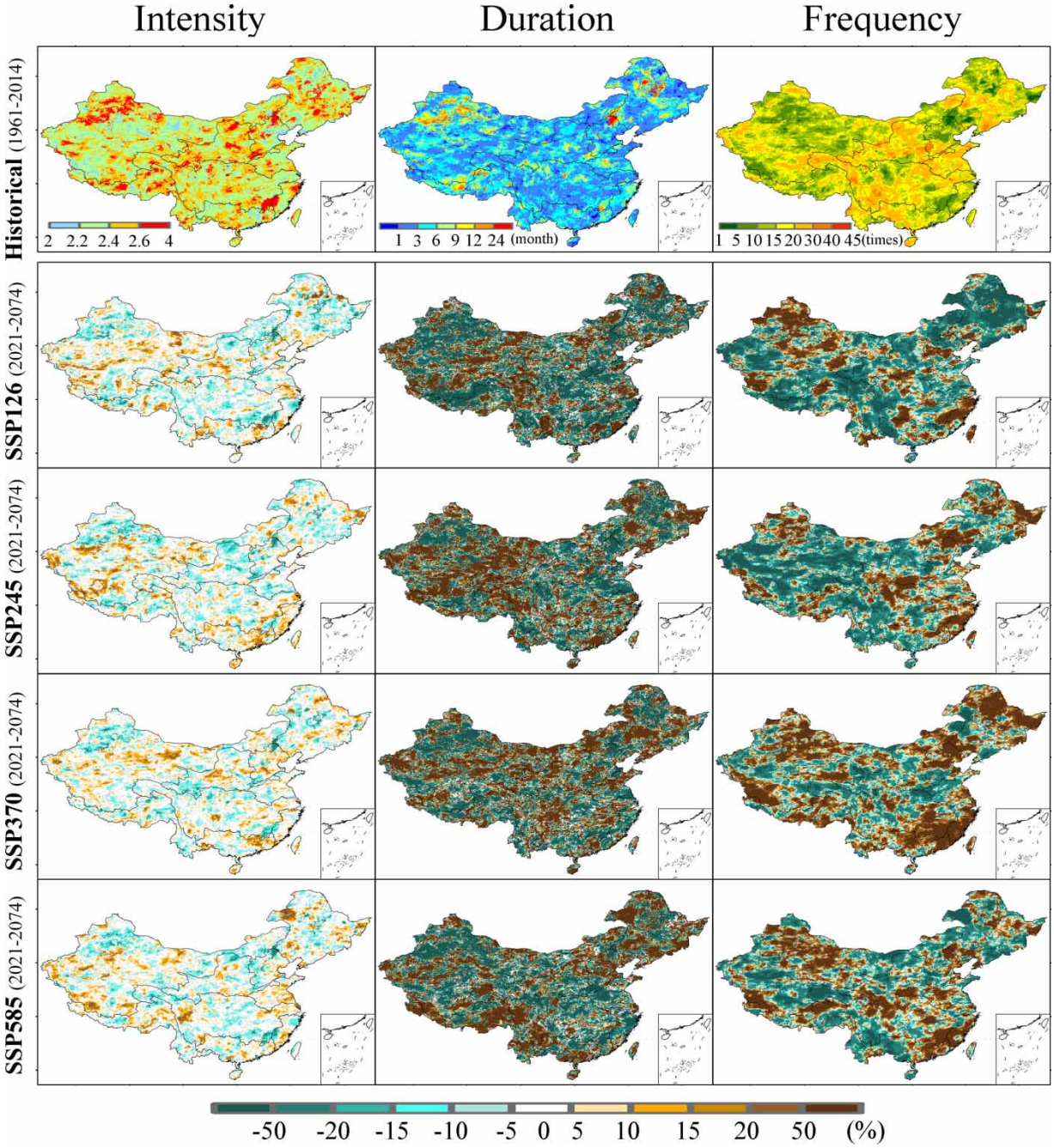

Figure 5 | Intensity median value and duration median value of drought events, as well as frequency of drought events during historical period (1961–2014). Percentage changes (2021–2074 minus 1961–2014) in drought intensity median, duration median and frequency under four scenarios.

characteristics. In historical period, the probability distribution of drought intensity shows a relatively linear change. However, in the future period, the probability is a fixed value of 0.1 when the drought intensity is between 1 and 2. The probability distribution of drought intensity shows a linear change when the drought intensity is greater than 2. For a given drought duration, the probability of drought occurrence in the historical period is less than that in the future period.

Overall, there is a large difference in the range of probability variation of drought duration and drought intensity under the two drought return periods. Compared with historical periods, the value of drought intensity in the future period is larger for a

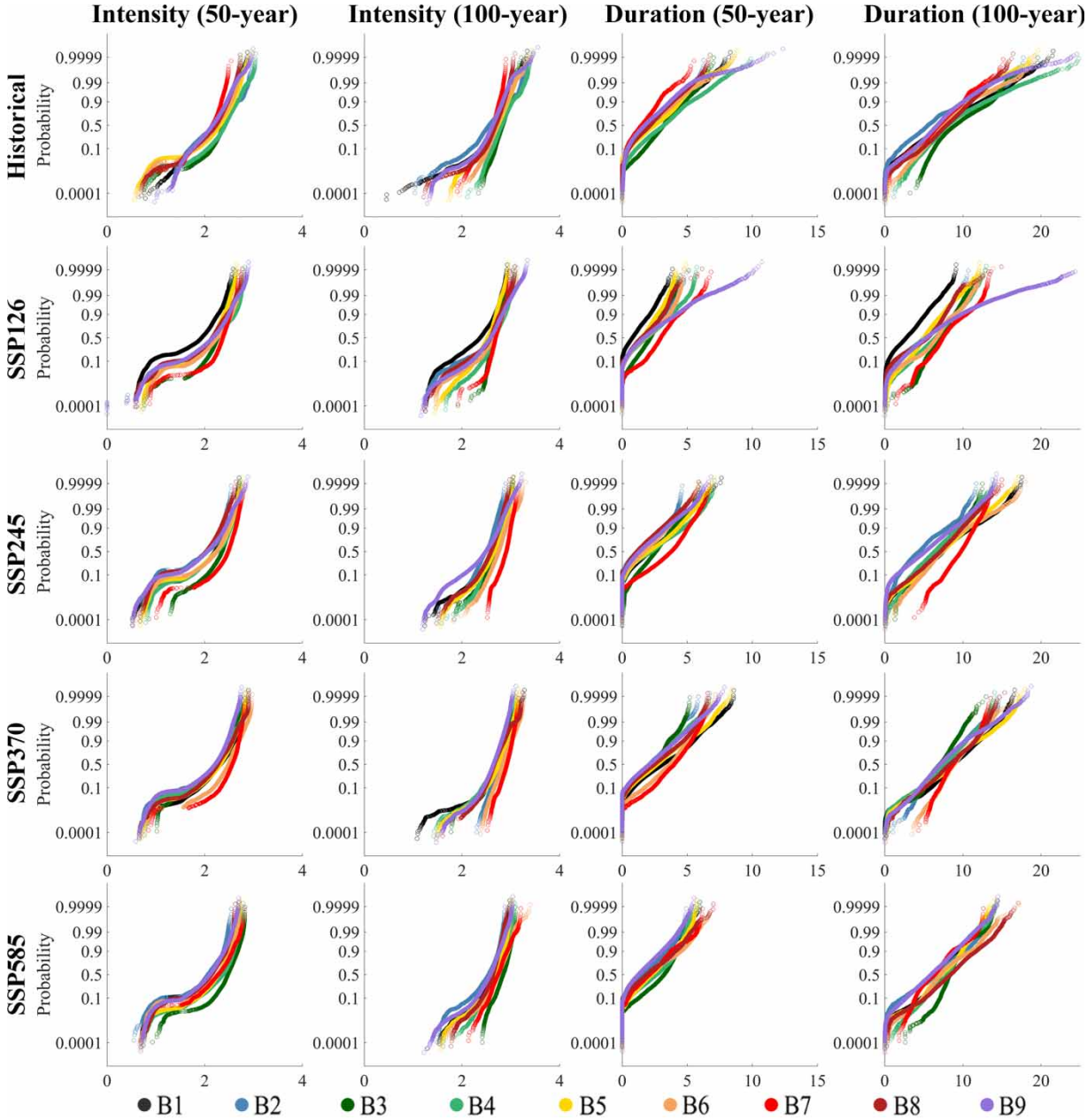

Figure 6 | Probability plot of return period (month) for intensity and duration under 50-year and 100-year drought levels (the unit of *x*-axis is month for duration and intensity in no units) in nine basins.

certain probability level. Meanwhile, the probability change rates of drought intensity and duration are different and the univariate drought risk analysis is not comprehensive enough. Therefore, instead of focusing on a single characteristic of drought, we should incorporate multiple drought risk evaluation indicators.

Second, we used the copula method to carry out a multifactor drought risk assessment by combining drought duration and intensity. We selected four couple distributions (Clayton copula, Gaussian copula, Gumbel copula and Frank copula) and three evaluation indices (Mean Square Error (MSE)), RMSE and Pearson Correlation Coefficient (R)) to optimize the distribution. The fitting distributions of the above two drought characteristics in nine river basins in China were evaluated. As seen from the evaluation results, the joint distribution effect of the Frank copula function was the best. Therefore, this study applied the Frank copula function as the joint distribution function in all river basins.

Figure 7 represents the JRP and RP of drought intensity and duration under different univariate return periods ($T = 50$ years and $T = 100$ years). The results show that the JRP and RP of drought intensity and duration of the four future scenarios demonstrate minimal change during the historical period in the central inland basin (B4 and B5) and the coastal southern basin (B3, B6 and B7). For the northeast basin (B1 and B2) and the western basin (B8 and B9), the JRP in the future period was larger than that in the historical period and the RP was smaller than that in the historical period under the 50-year drought levels; the results were most prominent under the SSP126 and SSP245 scenarios. Therefore, the degree of meteorological drought disaster in inland basins (B4 and B5) is expected not to change significantly in the future. For the 50-year drought levels with low drought severity, future meteorological droughts in the western and northeast basins are significantly affected by low and medium emission scenarios (SSP126 and SSP245). However, the JRP and RP of future drought intensity and duration varied significantly under the SSP126 and SSP370 scenarios compared with historical periods under 100-year drought levels.

4.4. Meteorological variables associated with meteorological drought

Meteorological droughts are influenced by meteorological variables. To explore the influence of meteorological variables on meteorological droughts, we discuss and analyse both precipitation and temperature.

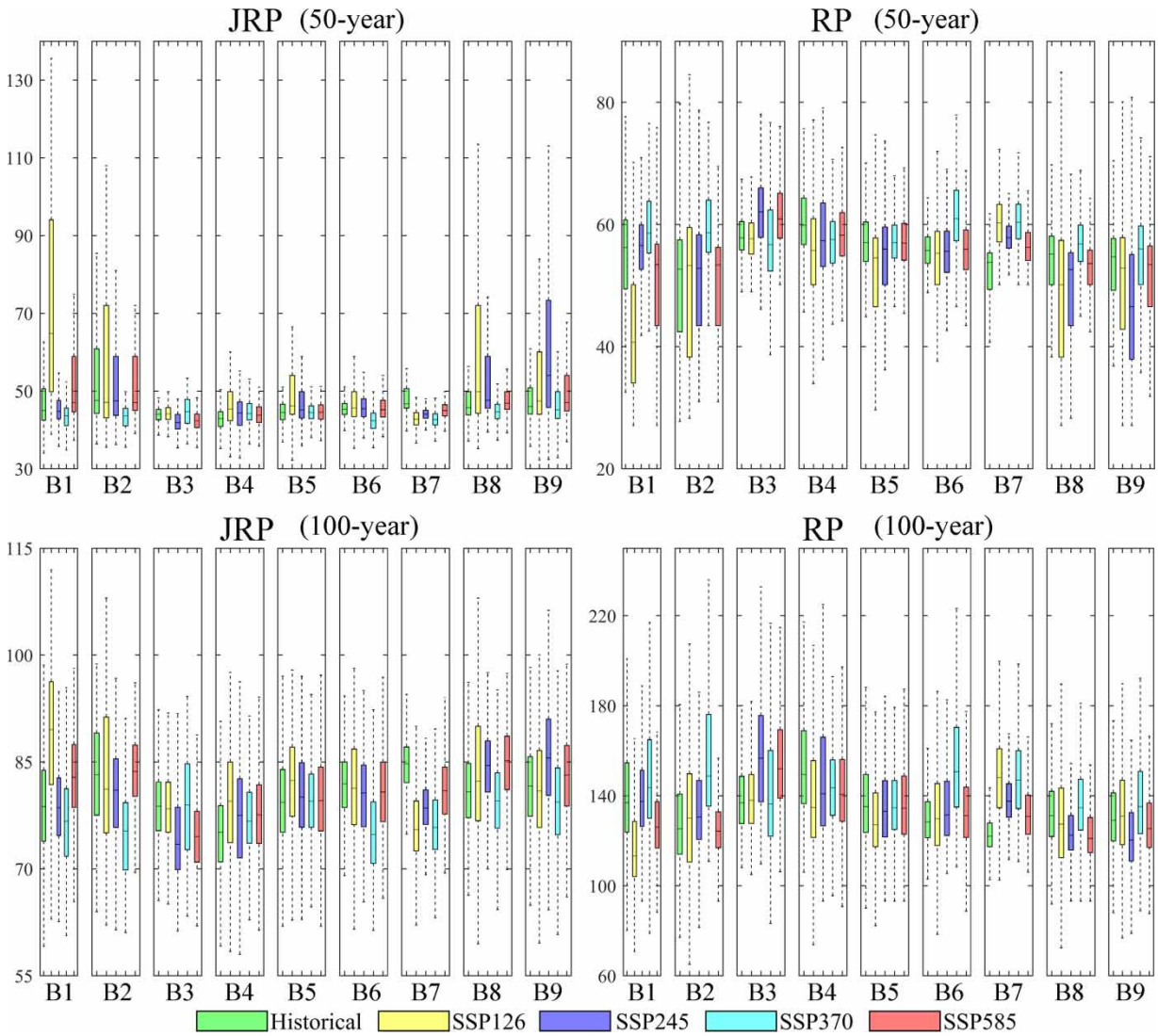

Figure 7 | JRP, RP of drought intensity and duration under 50-year and 100-year univariate return periods (unit: year) in nine basins.

In this study, we calculated precipitation and temperature anomaly values in the nine considered basins during historical (1961–2014) and future (2015–2098) periods under four emission scenarios and the reference period is the historical period. Figure 8 shows the variation curves of precipitation and temperature anomaly values in nine river basins. The overall trends of precipitation and temperature anomaly values increase in the future, the precipitation and temperature anomaly values of the high emission scenario (SSP585) are the largest and the temperature anomaly is clear. With the level increase of emission scenarios, the temperature anomaly values also increase. There is no clear regional difference in the temperature anomaly, but there is a substantial difference in the precipitation anomaly among different basins. In the eastern coastal basins (B2, B3, B6 and B7), the precipitation anomaly fluctuates greatly from 2021 to 2074, while in the other basins, the precipitation anomaly shows a steady increasing trend. In the southern coastal basins (B6 and B7), the precipitation anomaly under the SSP370 emission scenario is significantly smaller than that under the other emission scenarios. This shows that the variation in temperature variables is relatively stable, while the variation in precipitation anomalies in different basins is more complex and the regional difference in precipitation variables is large.

To reveal the detailed linkages between meteorological variables and meteorological drought intensity, we selected the wavelet coherence method (Torrence & Webster 1999). Meteorological variables include annual precipitation anomalies and annual temperature anomalies. The covarying relationship between the annual precipitation anomaly series and annual drought intensity is depicted in Figure 9. Figure 10 shows the relation between the temperature anomaly series and annual drought intensity. By comparing Figures 9 and 10, the results show that the covarying relationship between precipitation and drought intensity is significantly higher than that of temperature. From 1961 to 2014, the wavelet coherence of precipitation and drought intensity had significant covariance in the 4–16 years band (see the thick contour in Figure 9), except for the southern basins (B5–B7). From 1970 to 1980, significant coherence of approximately 0.85–0.9 within the 6–8 years band shows an in-phase difference of approximately 20°–90°. The significant correlation between precipitation and drought intensity during the future period is obviously lower than that of the historical period. Additionally, for the southeast coastal watersheds (B6 and B7), the correlation between precipitation under the SSP370 emission scenario in the future and drought intensity is more significant within the 6–16 years band.

The covarying relationship between temperature and drought intensity is significantly correlated with low emissions in the future period and significant coherence within the 0–4 years band shows an in-phase difference of 10°–90° (Figure 10). The results show that precipitation is the main influencing factor of meteorological drought, with the most significant correlation in the historical period and mainly occurs in the northern basin (B1), the central basins (B2–B4) and the western basins (B8–B9). In the future, the areas with a significant correlation between precipitation and drought intensity are mainly concentrated in northeast basins (B1–B3) and southeast coastal basins (B6–B7). In particular, the correlation is more prominent under the higher emission scenario.

5. DISCUSSION

5.1. Meteorological drought driven by precipitation or temperature

Meteorological drought is influenced by many factors and among the meteorological factors, precipitation and temperature dominate. The results in Section 4.3 show that precipitation appears to have a more pronounced effect on meteorological drought than the temperature in China. There have been many studies on the drivers of meteorological drought in other countries around the world. For example, in the midlands of the UK, Rahmani & Fattahi (2021) found that using nonlinear dynamics and cross-correlation, precipitation has a greater effect on meteorological droughts than temperature. This indicates that meteorological droughts are more sensitive to precipitation fluctuations than to temperature fluctuations. However, whether precipitation is the main driver of a meteorological drought depends on the actual precipitation situation in the study area. For example, Spinoni *et al.* (2015) found that in Central Europe and the Balkans, precipitation did not increase significantly and temperature drives the increase in meteorological drought severity. However, in Northern and Eastern Europe, although there has been a marked increase in temperature, the significant increase of precipitation leads to a decrease in drought characteristics (Spinoni *et al.* 2015). Therefore, whether meteorological drought is driven by precipitation or temperature mainly depends on the degree of precipitation decrease or temperature increase. In China, Liu *et al.* (2016) also found that the Precipitation–Concentration Degree (PCD) is significantly correlated with meteorological drought. Results show that the higher the PCD, the longer the duration of drought and more frequently the drought occurred. Therefore, precipitation has a significant impact on meteorological drought in China. There were a few limitations regarding our analysis on

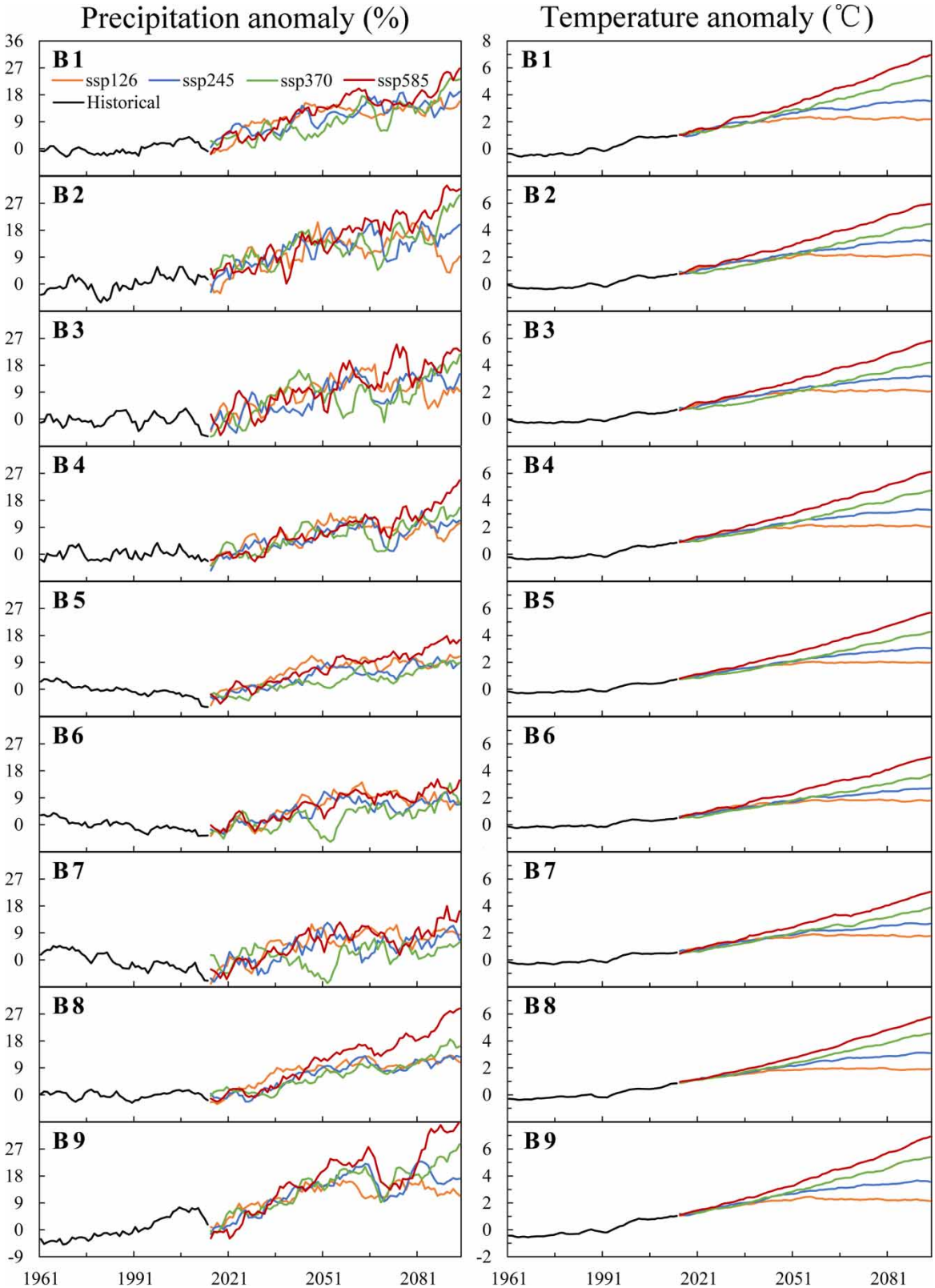

Figure 8 | Time series of precipitation and temperature anomalies in historical period (from 1961 to 2014) and future period (from 2015 to 2098) for nine basins.

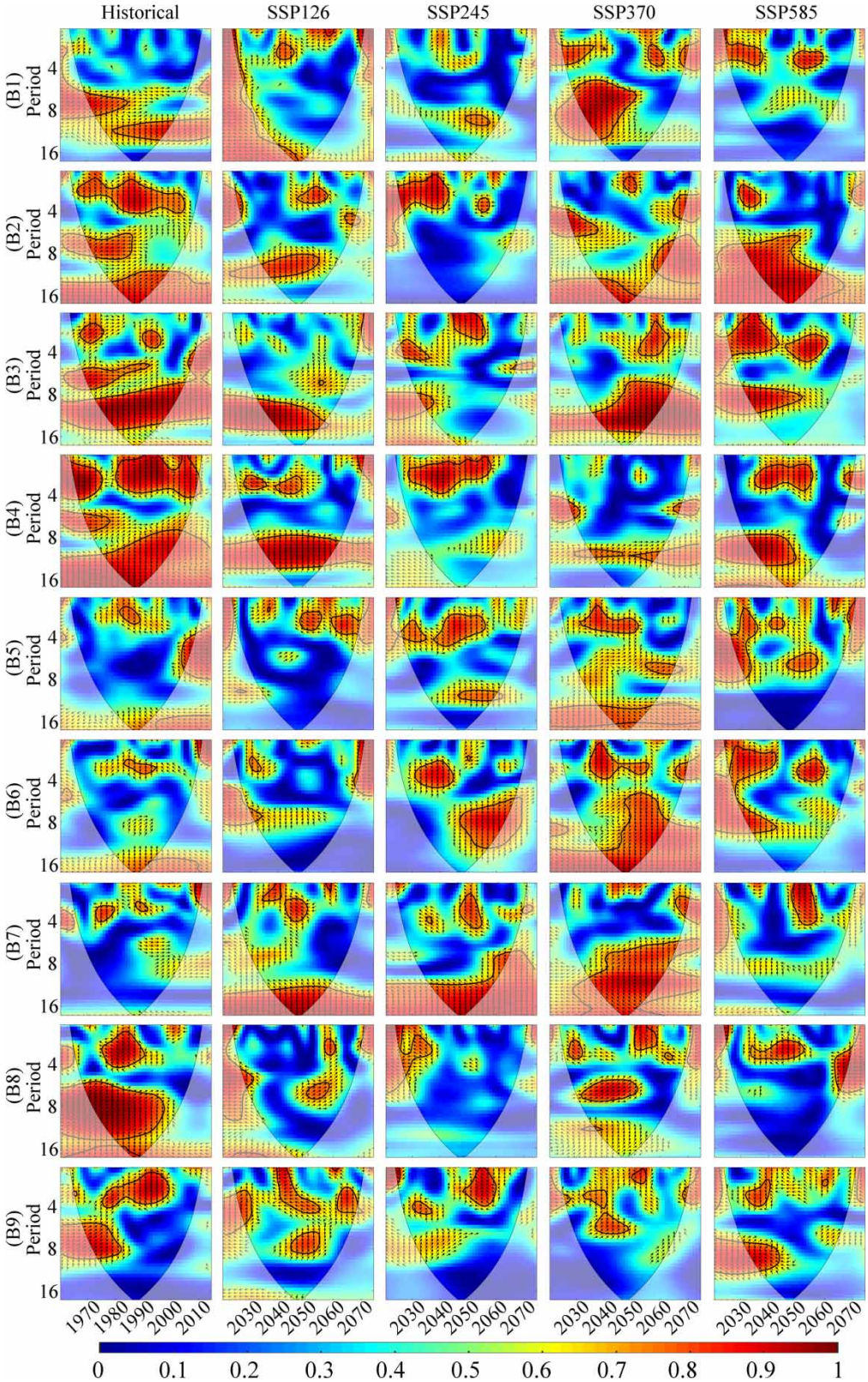

Figure 9 | The wavelet coherence between the annual precipitation anomaly and the corresponding annual drought intensity during historical (1961–2014) and future (2021–2074) periods in nine basins. (The 95% confidence level against red noise is exhibited as a thick contour and the relative phase relationship is denoted as arrows (with in-phase pointing right, anti-phase pointing left.)

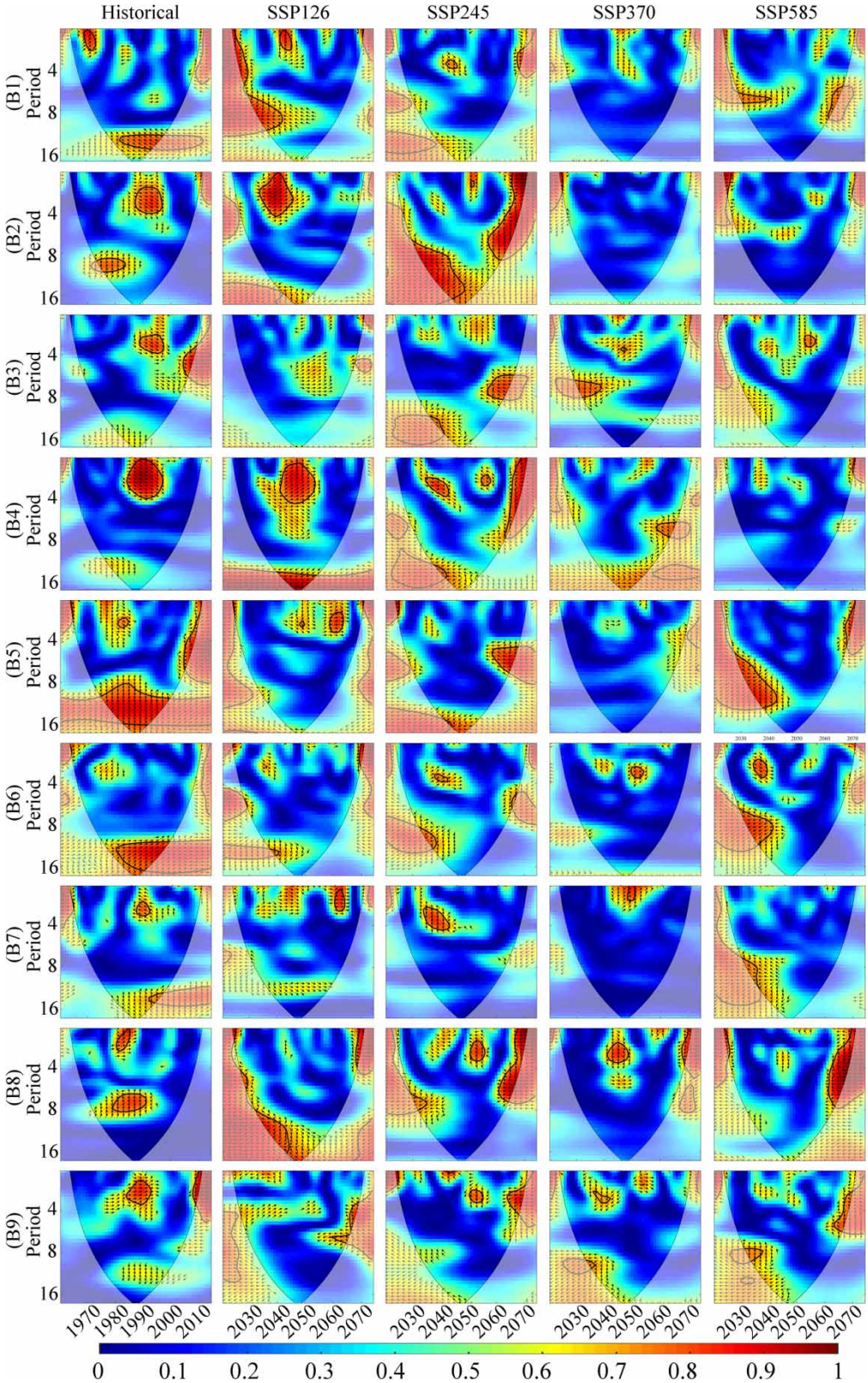

Figure 10 | The wavelet coherence between the temperature anomaly and the corresponding annual drought intensity during historical (1961–2014) and future (2021–2074) periods in nine basins. (The 95% confidence level against red noise is exhibited as a thick contour and the relative phase relationship is denoted as arrows (with in-phase pointing right, anti-phase pointing left.)

the drivers of meteorological drought, we did not consider other parameters, such as evapotranspiration, wind speed and sunshine. Next, we will consider a variety of meteorological factors and explore their impacts on meteorological drought.

5.2. Future projection uncertainties from CMIP6

Through bias correction, the CMIP6 model has significantly improved the simulation of precipitation and temperature, but it still has significant uncertainties. The uncertainty of CMIP6 directly affects the assessment accuracy of meteorological drought. Recently, uncertain studies on CMIP6 usually focused on temperature factors (You *et al.* 2021) and researches on the uncertainty of precipitation variables in CMIP6 mostly focus on extreme precipitation (Xu *et al.* 2022). Therefore, we discussed the uncertainty associated with CMIP6 in terms of precipitation and temperature and explored the differences at the basin scale. There are three main sources of uncertainty in climate projection: internal variability, model uncertainty and scenario uncertainty (Hawkins & Sutton 2011). We analysed the uncertainties in precipitation and temperature from CMIP6 in different basins. According to the uncertainty method (Hawkins & Sutton 2011), 15 CMIP6 climate models (Table 1) and four scenarios (SSP126, SSP245, SSP370 and SSP585) were selected to isolate and quantify sources of uncertainty in CMIP6. Figure 11 shows the fractional uncertainty in decadal annual precipitation and annual mean temperature over China. In the nine considered basins, there are the total variability and fractional uncertainty of three sources.

For the temperature variable in China, total uncertainty will initially decrease and then increase in the future (2021–2074), reaching its minimum in approximately 2040. Model uncertainty and scenario uncertainty of temperature impact total fractional uncertainty. This conclusion is consistent with the research results of You *et al.* (2021). As time progresses, the total fractional uncertainty of precipitation will decrease, which dominates the contributions from the model and internal variability. This feature is also found in the global CMIP6 uncertainty study (Zhang & Chen 2021). This shows that the main contribution of temperature and precipitation uncertainty comes from model uncertainty, among the three sources of uncertainty. Meanwhile, model uncertainty shows clear regional differences. Model uncertainties in northern basins (B1–B4) and western basins (B8–B9) have the greatest impacts. Therefore, in the application of CMIP6 in China, the CMIP6 model should be carefully selected to reduce the simulation error caused by CMIP6. In addition, the correction method of climate model dataset also has a significant impact on model uncertainty. At present, there are many correction methods for climate models and there are certain errors in different correction results. The corrected errors will also be transferred to the model uncertainty. Therefore, in addition to the selection of climate models, the selection of correction methods should also be emphasised.

6. CONCLUSION

This research investigated the spatio-temporal evolution and the future risk of meteorological drought over nine river basins in China based on the bias-corrected CMIP6 model outputs. The drought risk was projected based on copula of probabilistic

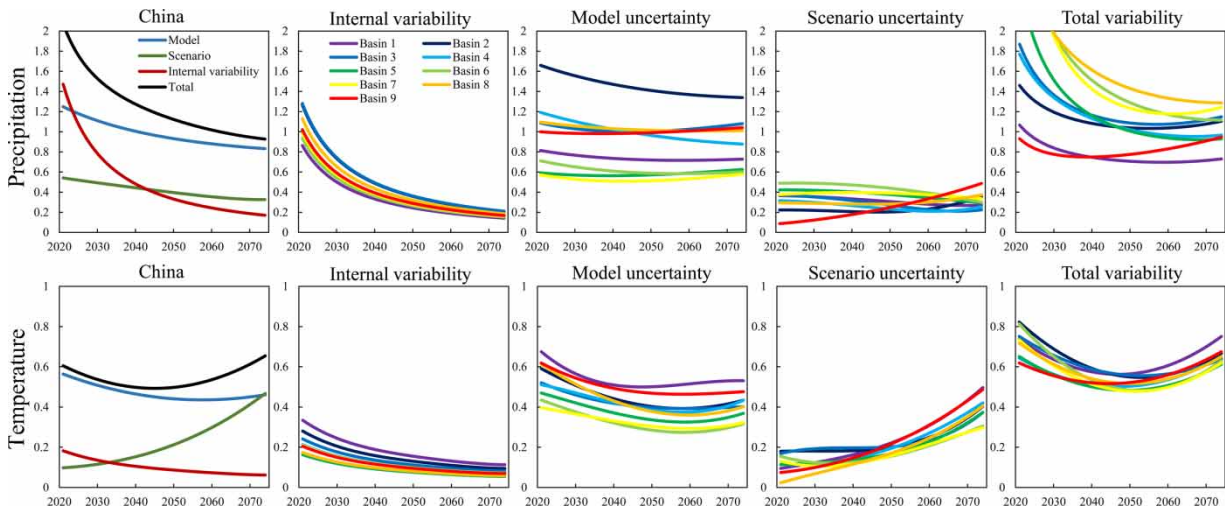

Figure 11 | The fractional uncertainty in decadal mean projections in China and nine basins.

multivariate drought characteristics. The results show a significant increasing trend of drought intensity and duration in the Northwest River, Southwest River and Songliao River Basins under four SSP scenarios (SSP126, SSP245, SSP370 and SSP585). The low and medium emission scenarios have more volatile drought risks than the others. Meanwhile, the driving factors of a meteorological drought are affected by the climatic characteristics and the precipitation is the most important factor in most basins in China.

Although the bias-corrected CMIP6 models perform well in China, model uncertainty is substantial in both temperature and precipitation, which can be transmitted from climate pattern to drought risk. The adoption of GCMs could introduce some uncertainties into drought prediction, we should explore the uncertainties in future drought work and it is a necessary aspect that could be better understood. Quantifying the uncertainty in drought risk from CMIP6 will reduce the impact of uncertainty in the drought risk projection.

This study provided a high-precision dataset of CMIP6 at 10 km spatial resolution, which is conducive to couple GCMs and hydrological models in hydrological process analysis. Focusing on the meteorological drought CMIP6 projections, our study could provide a reference for evaluating the drought recognition ability of CMIP6, especially in different river basins in China. In order to reduce the potential impacts of drought, future trends of drought need to be fully understood to lay the foundation for drought adaptation and mitigation strategies.

ACKNOWLEDGEMENT

The authors express our gratitude to Ming Pan (The Scripps Institution of Oceanography) for helpful discussions, and we thank the China Meteorological Administration (CMA) and the Program on Climate Model Diagnosis and Intercomparison (PCMDI) for making available the meteorological station datasets and CMIP6 models datasets. The authors acknowledge the support of the National Natural Science Foundation of China. We also thank the editors and reviewers for their efforts on this manuscript.

AUTHOR CONTRIBUTIONS

All authors contributed to the study conception and design. Material preparation, data collection and analysis were performed by Mengru Zhang and Linyan Zhang. The first draft of the manuscript was written by Mengru Zhang. All authors commented on previous versions of the manuscript. All authors read and approved the final manuscript.

FUNDING

This work was supported by the General Project of the National Natural Science Foundation of China (Grant No. U2243203, 52079036 and 42071040).

DATA AVAILABILITY STATEMENT

All relevant data are included in the paper or its Supplementary Information.

CONFLICT OF INTEREST

The authors declare there is no conflict.

REFERENCES

Bock, L., Lauer, A., Schlund, M., Barreiro, M., Bellouin, N., Jones, C., Meehl, G. A., Predoi, V., Roberts, M. J. & Eyring, V. 2020 Quantifying progress across different CMIP phases with the ESMValTool. *Journal of Geophysical Research: Atmospheres* **125** (21), 1–28.

Gräler, B., Van Den Berg, M. J., Vandenberghe, S., Petroselli, A., Grimaldi, S., De Baets, B. & Verhoest, N. E. C. 2013 Multivariate return periods in hydrology: a critical and practical review focusing on synthetic design hydrograph estimation. *Hydrology and Earth System Sciences* **17** (4), 1281–1296.

Gustavsson, J. & Peetre, J. 1977 Interpolation of Orlicz spaces. *Studia Mathematica* **60** (1), 33–59.

Hao, Z. & Singh, V. P. 2015 Drought characterization from a multivariate perspective: a review. *Journal of Hydrology* **527**, 668–678.

Harris, I., Jones, P. D., Osborn, T. J. & Lister, D. H. 2014 Updated high-resolution grids of monthly climatic observations – the CRU TS3.10 dataset. *International Journal of Climatology* **34** (3), 623–642.

Hawkins, E. & Sutton, R. 2011 The potential to narrow uncertainty in projections of regional precipitation change. *Climate Dynamics* **37** (1), 407–418.

Hayes, M., Svoboda, M., Wall, N. & Widhalm, M. 2011 The lincoln declaration on drought indices: universal meteorological drought index recommended. *Bulletin of the American Meteorological Society* **92** (4), 485–488.

Heim, R. R. 2002 A review of twentieth-century drought indices used in the United States. *American Meteorological Society* **83** (8), 1149–1165.

Huang, S., Huang, Q., Leng, G. & Liu, S. 2016 A nonparametric multivariate standardized drought index for characterizing socioeconomic drought: a case study in the Heihe River Basin. *Journal of Hydrology* **542**, 875–883.

IPCC 2021 *Climate Change 2021 The Physical Science Basis Summary for Policymakers Working Group I Contribution to the Sixth Assessment Report of the Intergovernmental Panel on Climate Change*.

Li, H., Sheffield, J. & Wood, E. F. 2010 Bias correction of monthly precipitation and temperature fields from Intergovernmental Panel on Climate Change AR4 models using equidistant quantile matching. *Journal of Geophysical Research Atmospheres* **115** (10), 1–20.

Li, C., You, S. & Wu, Y. 2020 Drought characteristics and dominant meteorological factors driving drought in spring maize growing season in northeast China. *Transactions of the Chinese Society of Agricultural Engineering* **36** (19), 97–106.

Liu, Y., Yan, J. & Cen, M. 2016 The relationship between precipitation heterogeneity and meteorological drought/flood in China. *Journal of Meteorological Research* **30** (5), 758–770.

Massey, F. J. 1951 The Kolmogorov-Smirnov test for goodness of fit. *Journal of the American Statistical Association* **46** (253), 68–78.

Mckee, T. B., Doesken, N. J. & Kleist, J. 1993 The relationship of drought frequency and duration to time scales. In: Preprints Eighth Conference on Applied Climatology, American Meteorological Society, Anaheim, CA, 17–22 January 1993.

Mishra, A. K. & Singh, V. P. 2011 Drought modeling – a review. *Journal of Hydrology* **403** (1–2), 157–175.

Na, Y., Fu, Q. & Kodama, C. 2020 Precipitation probability and its future changes from a global cloud-resolving model and CMIP6 simulations. *Journal of Geophysical Research: Atmospheres* **125** (5), 1–23.

Palmer, W. C. 1965 Meteorological Drought *U.S. Weather Bureau, Res. Pap. No. 45*. p.58. Available from: https://www.ncdc.noaa.gov/temp-and-precip/drought/docs/palmer.pdf.

Rahmani, F. & Fattahi, M. H. 2021 A multifractal cross-correlation investigation into sensitivity and dependence of meteorological and hydrological droughts on precipitation and temperature. *Natural Hazards* **109** (3), 2197–2219.

Samaniego, L., Thober, S., Kumar, R., Wanders, N., Rakovec, O., Pan, M., Zink, M., Sheffield, J., Wood, E. F. & Marx, A. 2018 Anthropogenic warming exacerbates European soil moisture droughts. *Nature Climate Change* **8** (5), 421–426.

Shukla, S. & Wood, A. W. 2008 Use of a standardized runoff index for characterizing hydrologic drought. *Geophysical Research Letters* **35** (2), 1–7.

Spinoni, J., Naumann, G., Vogt, J. & Barbosa, P. 2015 European drought climatologies and trends based on a multi-indicator approach. *Global and Planetary Change* **127**, 50–57.

Torrence, C. & Webster, P. J. 1999 Interdecadal changes in the ENSO-monsoon system. *Journal of Climate* **12** (8 PART 2), 2679–2690.

Vicente-Serrano, S. M., Beguería, S. & López-Moreno, J. I. 2010 A multiscalar drought index sensitive to global warming: the standardized precipitation evapotranspiration index. *Journal of Climate* **23** (7), 1696–1718.

Webb, R., Rosenzweig, C. E. & Levine, E. R. 2000 *Global Soil Texture and Derived Water-Holding Capacities (Webb et al.)*. ORNL DAAC, Oak Ridge, Tennessee, USA. https://doi.org/10.3334/ORNLDAAC/548. 2000. ORNL Distributed Active Archive Center.

Wells, N., Goddard, S. & Hayes, M. J. 2004 A self-calibrating palmer drought severity index. *Journal of Climate* **17** (12), 2335–2351.

Xu, H., Chen, H. & Wang, H. 2022 Future changes in precipitation extremes across China based on CMIP6 models. *International Journal of Climatology* **42** (1), 635–651.

Yang, X., Zhang, L., Wang, Y., Singh, V. P., Xu, C. Y., Ren, L., Zhang, M., Liu, Y., Jiang, S. & Yuan, F. 2020 Spatial and temporal characterization of drought events in China using the severity-area-duration method. *Water (Switzerland)* **12** (1), 1–16.

You, Q., Cai, Z., Wu, F., Jiang, Z., Pepin, N. & Shen, S. S. P. 2021 Temperature dataset of CMIP6 models over China: evaluation, trend and uncertainty. *Climate Dynamics* **57** (1–2), 17–35.

Yue, S., Yang, F. & Sheng, X. 2022 Spatiotemporal evolution and the driving factors of meteorological drought in the Hun-Taizi River Basin, NE China. *Journal of Water and Climate Change* **13** (3), 1326–1339.

Zhang, S. & Chen, J. 2021 Uncertainty in projection of climate extremes: a comparison of CMIP5 and CMIP6. *Journal of Meteorological Research* **35** (4), 646–662.

Zhang, M., Yang, X., Ren, L., Pan, M., Jiang, S., Liu, Y., Yuan, F. & Fang, X. 2021 Simulation of extreme precipitation in four climate regions. *Water* **13** (11), 1–17.

First received 1 December 2022; accepted in revised form 19 February 2023. Available online 8 March 2023